Asian Journal of Chemistry; Vol. 34, No. 7 (2022), 1814-1820

ASIAN JOURNAL OF CHEMISTRY

https://doi.org/10.14233/ajchem.2022.23776

Iron Capped Spent Tea Leaves as Nano-Adsorbent for Removal of Eriochrome Black T from Aqueous Phase

REHANA BAIJU MAMPILLY[1], AMANULLAKHAN PATHAN[2,*], CHETAN G. PRAJAPATI[3] and C.P. BHASIN[1]

[1]Department of Chemistry, Hemchandracharya North Gujarat University, Patan-384265, India
[2]Department of Chemistry, Shri Sarvajanik P.G. Science College, Mehsana-384001, India
[3]Department of Humanities and Science, Government Engineering College, Palanpur-385001, India

*Corresponding author: E-mail: amankhan255@gmail.com

Received: 22 February 2022; *Accepted*: 21 April 2022; *Published online*: 15 June 2022; AJC-20860

In present study, the removal of Eriochrome black T dye by iron nanoparticles prepared through tea leaves extract has been investigated. Synthesized iron capped nanoparticles were characterized by FTIR spectroscopy, X-ray diffraction (XRD), high-resolution transmission electron microscopy (HR-TEM) and field emission gun scanning electron microscopy (FEG-SEM) with EDAX. The X-ray diffraction patterns revealed that iron nanoparticles exhibited an amorphous nature. Scanning electron microscopy exhibited clearly spherical shape of iron nanoparticles. The transmission electron microscopy (HR-TEM) of iron nanoparticles shows the particle size in the range of 30-40 nm. Further, the degradation of Eriochrome black T dye was studied. To obtain the optimal conditions for the dye degradation, the effect of various experimental parameters, like the proportion of adsorbent, pH, the concentration of dye and contact time on the rate of reaction was studied. Adsorptions of Eriochrome black T dye follow pseudo-first-order kinetics. It was found that the dye degradation showed best results in the presence of sunlight at a pH of 3, Eriochrome black T dye concentration 50 ppm with 0.60 g of adsorbent. At 29 ± 1 ºC, the maximum removal of dye was achieved within 90 min.

Keywords: Adsorption, Iron nanoparticles, Tea leaves extract, Eriochrome black T dye.

INTRODUCTION

Environmental contamination is one of the most serious issues confronting the modern society today. Textile dyeing accounts for a significant portion of the industry and contaminates a substantial volume of water with dyes at various stages of the dyeing and finishing processes. Other industries that use dyes in a variety of processes include pulp mills, cosmetics, paper, printing, food, leather, *etc*. [1]. According to reports, various firms throughout the world create 7.0×10^5 tonnes of 10,000 distinct types of dyes on a yearly basis. During the dyeing process, around 1-15% of these colours are lost as effluents [2]. Dyes are synthetic colourants of organic origin that are responsible for both surface and groundwater pollution [3], as well as carcinogenic and mutagenic consequences [4]. Some synthetic colours are resistant to natural biodegradation and can be extremely hazardous to aquatic life. By obstructing sunlight, they can limit the photosynthetic activity of water plants. This situation may impair water re-oxygenation, affecting the proper growth of aquatic species [5].

Azo dyes generally account for over 70% of all synthetic dyes consumed by the dyeing industry globally. One or more azo groups (-N=N-) operate as chromophores in the molecular structure of a reactive azo dye [6]. Furthermore, molecules containing the azo group constitute the majority of synthetic dyes and are difficult to breakdown even at low concentrations due to their resistance to light, heat, chemicals and microbial attacks [7]. As a result, the removal of such synthetic dyes has become critical prior to the release of waste industrial effluents into the environment's water. Many attempts have been undertaken to remove dyes from wastewaters utilizing commonly used processes such as photocatalytic degradation [8,9], photo-Fenton reaction [10], biodegradation, coagulation, solvent extraction, precipitation, membrane filtering and advanced oxidation processes [11,12]. Because of their larger surface area and better adsorption capacity, nanoparticles have been

regarded as the most efficient adsorbents [13]. Iron based nanoparticles (Fe NPs) have been employed in groundwater treatment and site remediation in recent years because they are efficient and have a bigger surface area [14]. Although Fe NPs can be easily synthesized by chemical and physical methods, the use of toxic chemical substances such as sodium borohydride, organic solvents, stabilizing, high energy consumption and dispersion agents are disadvantages of these procedures, which were not used in this study [15]. Synthesis of iron nanoparticles from waste tea extract is a greener method that has gained popularity due to its cost effectiveness and environmentally benign approach [16].

Conventional methods used to remove dyes from wastewater are photocatalytic degradation [17-19], biological treatment [20], chemical coagulation [21], cation exchange membranes [22], electrochemical degradation [23], chemical-biological degradation [24], photo-Fenton reaction [25] and advanced oxidization process [26]. These methods give good results but the preparation of the materials and the execution process is very exhausting. Also, many secondary pollutants like various oxidative intermediates are produced during the photocatalytic degradation and oxidative process are more toxic than their parent compound. On the other hand, adsorption techniques are simpler and easier to conduct and integrate on a large scale.

Previous research has been undertaken on the manufacture of magnetic nanoparticles from tea waste and their application for the removal of arsenic and nickel from aqueous solutions [27,28]. In current study, however, iron nanoparticles were generated from spent tea leaves extracts and used to remove Eriochrome black T dye from an aqueous solution, which differs from the published studies. Recently, iron nanoparticles synthesized using plant extract [16,28-33] and green tea leaves and black tea [27,34] but all the investigations were based on the synthesis of iron nanoparticles by green tea.

In present study, the removal of Eriochrome black T dye by iron nanoparticles prepared through tea leaves extract has been investigated. Synthesized iron capped nanoparticles were characterized by FTIR spectroscopy, X-ray diffraction (XRD), High-resolution transmission electron microscopy (HR-TEM) and Field emission gun scanning electron microscopy (FEG-SEM) with EDAX. Further, the degradation of Eriochrome black T dye in the presence of sunlight and without sunlight was also studied. To obtain the optimal conditions for the dye degradation, the effect of various experimental parameters, like the proportion of adsorbent, pH, the concentration of dye and contact time on the rate of reaction was studied.

EXPERIMENTAL

AR grade ferrous sulfate and Eriochrome black T (EBT) dye were used as received from the S.D. Fine Chemicals (India) and used without further purification. Fresh green and black tea leaves were purchased from the local market. All the solution were prepared in the double distilled water.

Synthesis of iron nanoparticles: The tea leaves extracts were prepared by adding 60 g tea into 1000 mL distilled water and heated for 60 min in a water bath and then the extract were vacuum-filtered. After cooling to the room temperature, then 0.10 mol/L $FeSO_4$ solutions was added to the tea extracts with a ratio volume of 1:2. The resulting solution was centrifuged for 20 min; the supernatant was discarded and washed three times with distilled water to remove unreacted salts and tea phytochemicals on the colloidal surface. After washing, the iron nanoparticles were centrifuged and the nanoparticles were dried in an oven.

Characterization: Synthesized iron nanoparticles were characterized by following various analytical techniques. Fourier transform infrared (FTIR) spectra of synthesized iron nanoparticles were recorded on a Shimadzu (IR Spirit) instrument in the range of 4000-400 cm^{-1} using KBr pellet technique. X-ray powder diffraction (XRD) analysis was carried out on a RigakuD/max40kV diffractometer equipped with the graphite monochromator and Cu target. Field emission gun scanning electron microscope (FEG-SEM) images were recorded on a JSM-7600F series instrument and high-resolution transmission electron microscope (HR-TEM) images were recorded on a Tecnai G2-F30 electron microscope. The sample preparation was carried out *via* the coating on carbon coated grid Cu Mesh 300 prior to the measurement. The adsorption properties of the synthesized iron nanoparticles were recorded by UV-1800, Shimadzu spectrophotometer.

Adsorption studies: The adsorption studies of the synthesized iron nanoparticles was assessed by monitoring decolourization of Eriochrome black T dye. Iron nanoparticles interacted with Eriochrome black T dye solution at different pH (2.0-10.0), different amount of adsorbent, different concentration of dye and contact time. The adsorption experiments were carried out in different conditions; for these experiments, the Eriochrome black T dye solution was placed in an equal amount in two beakers. (a) First beaker containing Eriochrome black T dye solution and iron nanoparticles at room atmosphere without sunlight; and (b) second beaker containing Eriochrome black T dye solution and iron nanoparticles was kept at sunlight.

The reaction temperature was kept constant at 29 ± 1 ºC using a circulating liquid bath. Before irradiation experiments, 200 mL of dye solution of appropriate concentration containing the desired quantity of adsorbent (0.1-1.0 g) and a predetermined amount of 2 mM NaOH solution and HCl (for pH), was magnetically stirred, while the solution was kept at least for 15 min in dark to attain adsorption-desorption equilibrium between the dye solution and the adsorbent surface.

Afterwards, the first sample (at 0 min) was taken out and the irradiation was started. During irradiation, about 5-10 mL were withdrawn at regular time (every 15 min) intervals, centrifuged and the supernatant was subsequently analyzed. The change in absorbance of the dye aliquots was followed at its λ_{max} (538 nm) as a function of irradiation time. The observed absorbance spectra were in agreement with Beer-Lambert's law in the range of examined dye concentration. The concentration of dye was calculated by a standard calibration curve obtained from the absorbance of the dye at different known concentrations. The adsorption experiments were repeated three times in order to check the reproducibility of the experimental results. The accuracy of the absorbance was found to

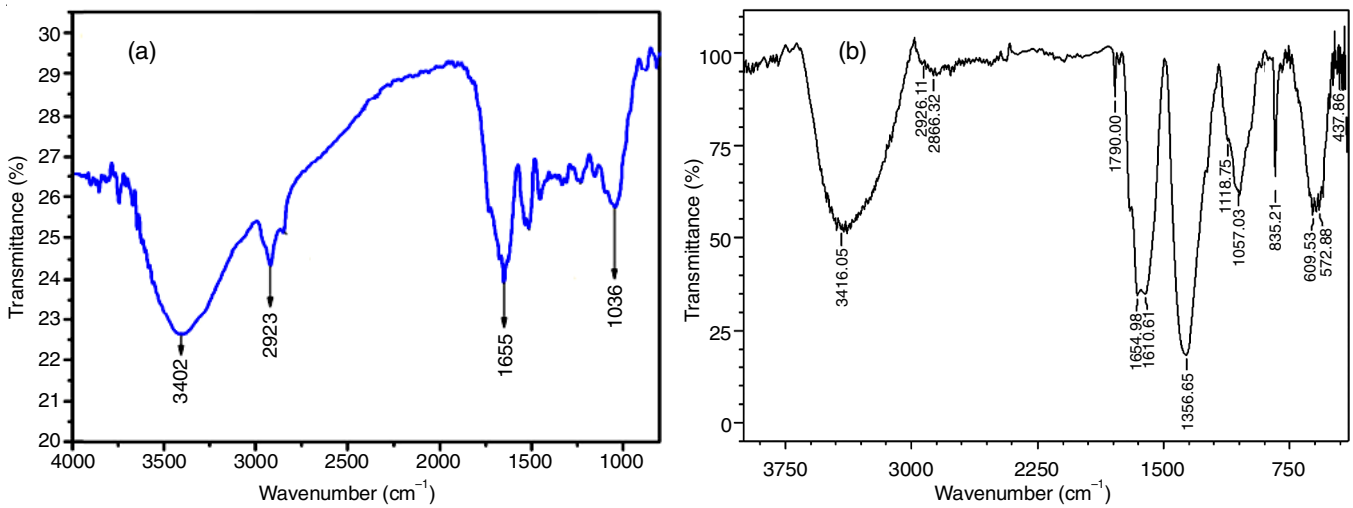

Fig 1. FTIR spectra of iron nanoparticles before (a) and after (b) adsorption of Eriochrome black T

be within ± 2. The consistency in the activity of the adsorbent was analyzed by the recycling experiments. After the first attempt of the adsorption experiment, the adsorbent was retrieved from the centrifugation. The retrieved adsorbent was thoroughly washed with deionized water and ethanol. The adsorbent was dried at 60 ºC for 12 h and then reused in the next cycle of the adsorption experiment. Equally, the experiment was repeated for a set of cycles to monitor the loss in efficiency of the adsorbent after repetitive use.

The removal efficiency (%) was calculated as follows:

$$\text{Degradation } (\%) = \frac{C_o - C}{C_o} \times 100 \quad (1)$$

where C_o is the initial concentration of Eriochrome black T dye and C is the time-dependent concentration of dye upon irradiation of visible light. The following first-order kinetic equation can be used to describe the removal of Eriochrome black T dye.

$$\ln\left(\frac{C_o}{C_t}\right) = kt \quad (2)$$

where C_o and C_t are the concentrations of dye in solution at times 0 and t, respectively and k is the first-order rate constant (s^{-1}).

RESULTS AND DISCUSSION

FTIR spectra of iron nanoparticles: The FT-IR spectrum (Fig. 1) reveals that Fe-capped spent tea leaves as nanoparticles contained a variety of functional groups. The bound –OH groups were represented by the broad band at 3402 cm^{-1}. The -C-C stretching of the alkane functional groups caused the peaks at 2923 and 2853 cm^{-1}. Similarly, the band about 1655 cm^{-1} could be attributed to the -C=C stretching vibration and aromatic functionality. The C-O and C=O groups were allocated to the two bands at 1146 and 1036 cm^{-1}, respectively [31-33].

X-ray diffraction (XRD) spectra of iron nanoparticles: Fig. 2 shows the XRD patterns of iron nanoparticles synthesized using tea extracts. The peaks observed in XRD patterns at 2θ

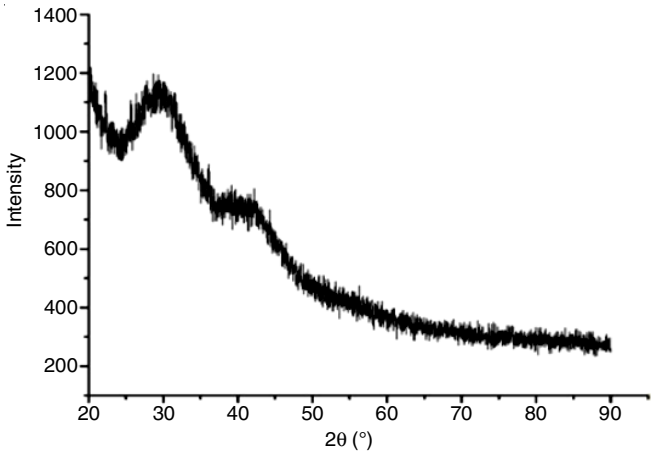

Fig. 2. X-ray diffraction spectra of iron capped tea leaves nanoparticles

values of 44.9º, 35.68º, 35.45ºand 20.35º corresponded to zero-valent iron (α-Fe), maghemite (α-Fe_2O_3), magnetite (Fe_3O_4) and iron hydroxides [35,36]. However, iron oxides and iron oxo hydroxides were mainly observed instead of Fe^0 because the iron nanoparticles synthesized by tea extract were amorphous in nature [16]. Intensity peak at 2θ = 21.56º was identified as the organic in gradient polyphenols/caffeine from tea extract [37,38].

FEG-SEM studies of iron nanoparticles: The surface morphology of the synthesized iron nanoparticles were examined by scanning electron microscopy. Fig. 3 shows the iron nanoparticles before reaction with Eriochrome black T, which confirmed that the iron nanoparticles have a spherical morphology with diameter ranges between 30-40 nm. The EDAX spectra of Fe capped nanoparticles show the peaks for iron and oxygen elements indicating the good development of Fe capped nanoparticles. Peak indexing of the elements is oxygen 0.5 keV and iron 6.4 and 7.2 keV. The compositions in the mass percentage of the elements are oxygen 30.53% and iron 62.72%.

HR-TEM studies of iron nanoparticles: Fig. 4 shows the HR-TEM micrograph of the synthesized iron nanoparticles. HR-TEM images showed that the majorities of particles were

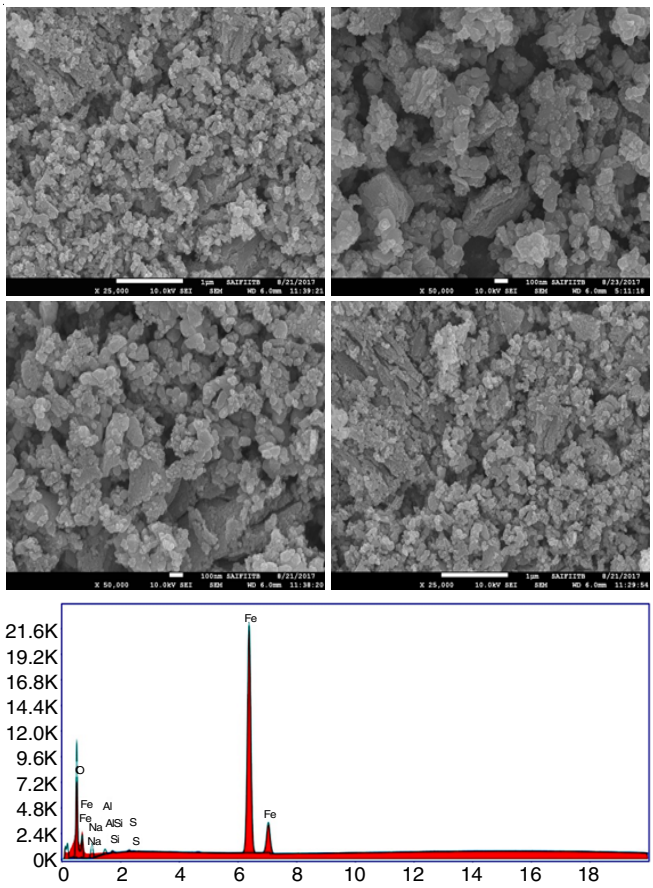

Fig. 3. FE-SEM of iron nanoparticles with EDAX

between 30-40 nm in size, possessed a circular morphology and uniform in shape. The crystallinity of Fe capped nanoparticles was demonstrated using a selected area electron diffraction (SAED) pattern with brilliant circular spots.

Optimization of adsorption parameters

Effect of adsorbent dosage: Because the amount of iron nanoparticles utilized is likely to alter the dye degradation process, different amounts of nanoparticles were used. When the amount of adsorbent dose was increased, the percentage of Eriochrome black T dye elimination likewise rose. This is due to the increased iron surface area and more accessible adsorption active site, however after adding a particular amount (0.60 g) of an adsorbent, the rate became practically constant (Fig. 5). This could be because, beyond a certain point, increasing the amount of adsorbent did not increase the adsorbent's exposed surface area (active sites). As the adsorbent covered the bottom of the reaction tank, it only increased the thickness of the layer. It is possible that a saturation point was reached and that after this saturation point, no effect of adsorbent quantity was detected.

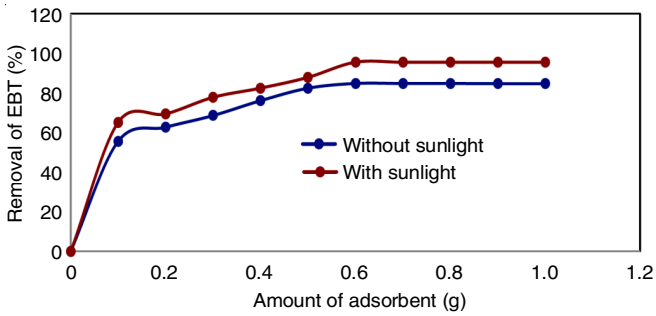

Fig. 5. Effect of adsorbent dosage on the adsorption of Eriochrome black T (EBT)by iron nanoparticles

This theory was also supported by the use of reaction containers of various sizes. As the bottom area of the vessel increased, so did the adsorbent exposed area and thus the percentage of dye removal increased. In the current study, beakers of the same size were used for the whole experiment and after a maximum exposure to adsorbent, additional adsorbent addition simply raised the layer thickness, but did not contribute to improving the percent of dye removal. According to the experimental results, 0.60 g of adsorbent was successful in achieving the greatest removal percentage in Eriochrome black T dye.

Effect of pH: Because the charge of a surface on adsorbent and dye molecules can be modified by pH values in aqueous solution, the initial pH value is one of the most important parameters influencing the removal process of dyes for water treatment. The experiments were carried out at a fixed adsorbate concentration (50 ppm), adsorbent dosage of 0.60 g and a temperature of 29 ± 1 ºC. The pH was altered by adding 0.1 M HCl or 0.1 M NaOH and the dye's adsorption was tested throughout a pH range of 2-10. Eriochrome black T is a cationic dye that exists in aqueous solution as positively charged ions. As a charged ion, the degree of its adsorption onto the surface

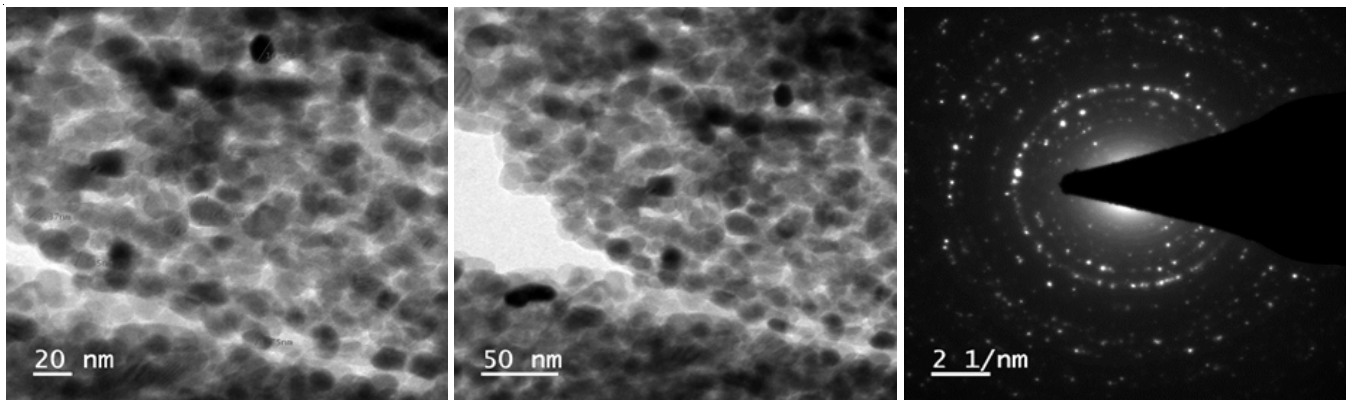

Fig. 4. HR-TEM images of iron nanoparticles

of iron nanoparticles is mostly affected by the adsorbent's surface charge, which is influenced by the solution pH.

Fig. 6 depicts the obtained results, which show that the adsorption of Eriochrome black T dye increases with increasing pH from 2.0 to 7.0 and that when pH increases further, the percent of removal of Eriochrome black T (EBT) begins to decrease. This is because the surface activities of the iron nanoparticles change from positive to negative charge when pH increases, resulting in electrostatic interaction between the adsorbent and Eriochrome black T molecules. As seen in Fig. 5, as the pH rises from 2 to 7, the proportion of dye removed rises and as the pH rises from 3 to 10, the removal percentage of dye decreases. At pH 3.0, iron nanoparticles absorbed the most Eriochrome black T dye. The maximal degradation of Eriochrome black T dye with iron nanoparticles was approximately 95.32%.

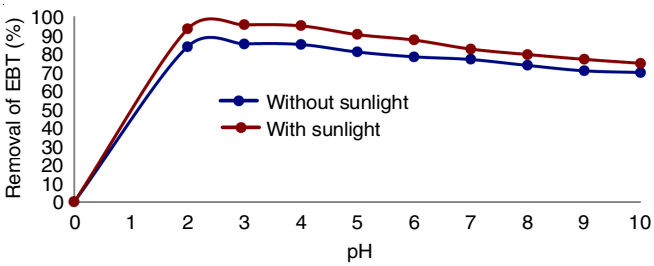

Fig. 6. Effect of pH on the adsorption of Eriochrome black T by iron-nanoparticle

Effect of dye concentration: The initial concentration of Eriochrome black T varied from 50 to 250 ppm. It has been discovered that as the initial Eriochrome black T concentration increases from 50 to 250 ppm, the equilibrium adsorption increases. The findings were due to the fact that when the initial concentration increases, the mass transfer driving force increases, resulting in the greater Eriochrome black T adsorption. It was also discovered that the percentage of dye removed decreases as the original concentration of Eriochrome black T dye increases. According to Fig. 7, the greatest dye removal by wasted tea leaves was 95.55% in a 50 ppm solution of Eriochrome black T.

Effect of contact time: The most essential parameter in adsorption dye removal is the influence of contact time. All of the experiments were carried out over a set period of time. Fig. 8 depicts the influence of contact time on the elimination

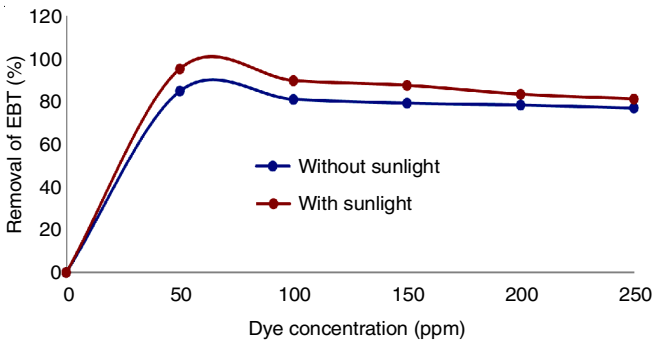

Fig. 7. Effect of concentration on the adsorption of Eriochrome black T by ironnanoparticles

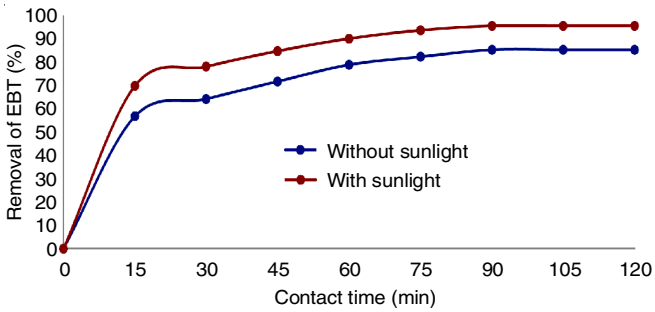

Fig. 8. Effect of contact time on the removal of Eriochrome black T by iron nanoparticles

of Eriochrome black T by adsorbent. It is apparent that the percentage of dye elimination increases as contact duration increases. The effects of contact time on the elimination of Eriochrome black T were investigated in a set time interval.

The availability of a significant number of unoccupied sites for Eriochrome black T adsorption can be attributed to the rapid adsorption at initial contact time, but the sluggish rate of dye adsorption could be related to slow pore diffusion of the dye into the bulk adsorbent. Maximum dye removal was achieved at 90 min utilizing iron nanoparticles, which was approximately 95.60% (Fig. 9).

Comparison studies: The comparison studies was carried out in order to compare the efficiency of the iron nanoparticles prepared through tea leaves extract with the other reported nanoadsorbents. Table-1 clearly shows the the iron nanoparticles prepared waste tea leaves extract exhibit the best removal efficiency of Eriochrome black T as compared to other reported adsorbent materials.

TABLE-1
COMPARATIVE DATA OF PHOTOCATALYTIC DEGRADATION OF
ERIOCHROME BLACK T DYE IN PRESENCE OF VARIOUS PHOTOCATALYSTS

Photo catalyst	Catalyst load	Degradation (%)	Ref.
β-Cyclodextrin coated Fe_3O_4 (10 ± 2 nm)	60 mg	Degradation (90%) with hydrogen peroxide	[39]
Tri doped TiO_2/CNT	0.1 g	66% Removal observed by TOC due to degradation and followed first order kinetics	[40]
ZnO	100 mg	Degradation (92%) in UV light	[41]
NiO-ZnO on nanozeolite		Degradation (85%) in UV sunlight	[42]
Rice hull-based activated carbon	2 g	93.14% Removal by adsorption	[43]
$CuFe_2O_4$, $CuMn_2O_4$, $MnZn_2O_4$	80 mg	97% Dye degradation	[44]
CuO	0.02 g	98% Degradation in 60 min followed first order kinetics	[45]
Fe capped tea leaves nanoparticles	0.6 g	Degradation achieved with sun light and without sunlight was found to be 95.60% and 84.8% respectively	Present work

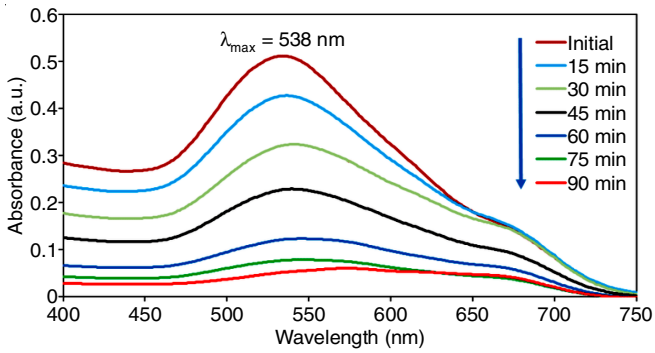

Fig. 9. UV-vis absorption spectra for degradation of Eriochrome black T (EBT) dye in the presence of Fe capped tea leaves nanoparticles

Conclusion

Iron nanoparticles produced from tea leaves extract were used to remove Eriochrome black T dye in aqueous phase. FTIR spectroscopy, X-ray diffraction (XRD), high-resolution transmission electron microscopy (HR-TEM) and scanning electron microscopy (FE-SEM) were used to characterize the synthesized iron nanoparticles. The X-ray diffraction patterns demonstrated that the iron nanoparticles were amorphous. The spherical shape of iron nanoparticles was readily visible using scanning electron microscopy. Transmission electron microscopy (HR-TEM) of iron nanoparticles revealed the particle sizes in the 30-40 nm range. Using iron nanoparticles, the degradation of Eriochrome black T dye was also monitored using visible absorption spectroscopy. The dye degradation performed best with in the presence of sunlight at different parameters likes pH of 3, Eriochrome black T dye concentration of 50 ppm and 0.60 g of adsorbent. By stirring for 90 min at 29±1 ºC, the maximal removal of the studied dye was obtained. Eriochrome black T dye adsorption followed the pseudo-first-order kinetics. The percentage of dye elimination using iron capped nanoparticles in the presence of sunlight and without sunlight was found to be 95.60% and 84.8%, respectively.

CONFLICT OF INTEREST

The authors declare that there is no conflict of interests regarding the publication of this article.

REFERENCES

1. P. Monvisade and P. Siriphannon, *Appl. Clay Sci.*, **42**, 427 (2009); https://doi.org/10.1016/j.clay.2008.04.013
2. N. Barka, M. Abdennouri and M.E. Makhfouk, *J. Taiwan Inst. Chem. Eng.*, **42**, 320 (2011); https://doi.org/10.1016/j.jtice.2010.07.004
3. N. Mohammadi, H. Khani, V.K. Gupta, E. Amereh and S. Agarwal, *J. Colloid Interface Sci.*, **362**, 457 (2011); https://doi.org/10.1016/j.jcis.2011.06.067
4. S.H. Lin, R.S. Juang and Y.H. Wang, *J. Hazard. Mater.*, **113**, 195 (2004); https://doi.org/10.1016/j.jhazmat.2004.06.028
5. A.N. Ejhieh and M. Khorsandi, *J. Hazard. Mater.*, **176**, 629 (2010); https://doi.org/10.1016/j.jhazmat.2009.11.077
6. A.A. Ahmad and B.H. Hameed, *J. Hazard. Mater.*, **175**, 298 (2010); https://doi.org/10.1016/j.jhazmat.2009.10.003
7. Ö. Gerçel, H.F. Gerçel, A.S. Koparal and Ü.B. Ögütveren, *J. Hazard. Mater.*, **160**, 668 (2008); https://doi.org/10.1016/j.jhazmat.2008.03.039
8. J. Sun, L. Qiao, S. Sun and G. Wang, *J. Hazard. Mater.*, **155**, 312 (2008); https://doi.org/10.1016/j.jhazmat.2007.11.062
9. J. García-Montaño, N. Ruiz, I. Munoz, X. Domenech, J.A. García-Hortal, F. Torrades and J. Peral, *J. Hazard. Mater.*, **138**, 218 (2006); https://doi.org/10.1016/j.jhazmat.2006.05.061
10. W. Azmi, R.K. Sani and U.C. Banerjee, *Enzyme Microb. Technol.*, **22**, 185 (1998); https://doi.org/10.1016/S0141-0229(97)00159-2
11. G. Crini, *Bioresour. Technol.*, **97**, 1061 (2006); https://doi.org/10.1016/j.biortech.2005.05.001
12. T. Robinson, B. Chandran and P. Nigam, *Water Res.*, **36**, 2824 (2002); https://doi.org/10.1016/S0043-1354(01)00521-8
13. M. Hua, S. Zhang, B. Pan, W. Zhang, L. Lv and Q. Zhang, *J. Hazard. Mater.*, **211-212**, 317 (2012); https://doi.org/10.1016/j.jhazmat.2011.10.016
14. L.N. Shi, X. Zhang and Z.L. Chen, *Water Res.*, **45**, 886 (2011); https://doi.org/10.1016/j.watres.2010.09.025
15. L. Huang, X. Weng, Z. Chen, M. Megharaj and R. Naidu, *Spectrochim. Acta A Mol. Biomol. Spectrosc.*, **117**, 801 (2014); https://doi.org/10.1016/j.saa.2013.09.054
16. T. Shahwan, S. Abu Sirriah, M. Nairat, E. Boyaci, A.E. Eroglu, T.B. Scott and K.R. Hallam, *Chem. Eng. J.*, **172**, 258 (2011); https://doi.org/10.1016/j.cej.2011.05.103
17. A.A. Pathan, K.R. Desai and C.P. Bhasin, *Curr. Nanomater.*, **2**, 169 (2018); https://doi.org/10.2174/2405461503666180420115141
18. S. Vajapara, S. Patel and C. Bhasin, *Int. J. Nano. Chem*, **3**, 33 (2017); https://doi.org/10.18576/ijnc/030203
19. K.R. Desai, A.A. Pathan and C.P. Bhasin, *Int. J. Nanomater. Chem.*, **3**, 39 (2017); https://doi.org/10.18576/ijnc/030204
20. A. Alinsafi, M. Da Motta, S. Le Bonté, M.N. Pons and A. Benhammou, *Dyes Pigments*, **69**, 31 (2006); https://doi.org/10.1016/j.dyepig.2005.02.014
21. H. Selcuk, *Dyes Pigments*, **64**, 217 (2005); https://doi.org/10.1016/j.dyepig.2004.03.020
22. J.S. Wu, C.H. Liu, K.H. Chu and S.Y. Suen, *J. Membr. Sci.*, **309**, 239 (2008); https://doi.org/10.1016/j.memsci.2007.10.035
23. L. Fan, Y. Zhou, W. Yang, G. Chen and F. Yang, *Dyes Pigments*, **76**, 440 (2008); https://doi.org/10.1016/j.dyepig.2006.09.013
24. G. Sudarjanto, B. Keller-Lehmann and J. Keller, *J. Hazard. Mater.*, **138**, 160 (2006); https://doi.org/10.1016/j.jhazmat.2006.05.054
25. B.H. Hameed and F.B.M. Daud, *Chem. Eng. J.*, **139**, 48 (2008); https://doi.org/10.1016/j.cej.2007.07.089
26. F.C. Wu and R.L. Tseng, *J. Hazard. Mater.*, **152**, 1256 (2008); https://doi.org/10.1016/j.jhazmat.2007.07.109
27. P. Panneerselvam, N. Morad and K.A. Tan, *J. Hazard. Mater.*, **186**, 160 (2011); https://doi.org/10.1016/j.jhazmat.2010.10.102
28. S. Lunge, S. Singh and A. Sinha, *J. Magn. Magn. Mater.*, **356**, 21 (2014); https://doi.org/10.1016/j.jmmm.2013.12.008
29. V. Smuleac, R. Varma, S. Sikdar and D. Bhattacharyya, *J. Membr. Sci.*, **379**, 131 (2011); https://doi.org/10.1016/j.memsci.2011.05.054
30. Y. Kuang, Q. Wang, Z. Chen, M. Megharaj and R. Naidu, *J. Colloid Interface Sci.*, **410**, 67 (2013); https://doi.org/10.1016/j.jcis.2013.08.020
31. O.V. Kharissova, H.R. Dias, B.I. Kharisov, B.O. Pérez and V.M.J. Pérez, *Trends Biotechnol.*, **31**, 240 (2013); https://doi.org/10.1016/j.tibtech.2013.01.003
32. V.V. Makarov, S.S. Makarova, A.J. Love, O.V. Sinitsyna, A.O. Dudnik, I.V. Yaminsky, M.E. Taliansky and N.O. Kalinina, *Langmuir*, **30**, 5982 (2014); https://doi.org/10.1021/la5011924
33. J. Lin, X. Weng, X. Jin, M. Megharaj, R. Naidu and Z. Chen, *RSC Adv.*, **5**, 70874 (2015); https://doi.org/10.1039/C5RA10629J

34. S.J. Patel, S. Vajapara and C.P. Bhasin, *Chem. Sci. Trans.*, 9, 35 (2020); https://doi.org/10.7598/cst2020.1710
35. Z.X. Chen, X.Y. Jin, Z. Chen, M. Megharaj and R. Naidu, *J. Colloid Interface Sci.*, **363**, 601 (2011); https://doi.org/10.1016/j.jcis.2011.07.057
36. Z.X. Chen, Y. Cheng, Z. Chen, M. Megharaj and R. Naidu, *J. Nanopart. Res.*, **14**, 1 (2012).
37. M. Colon and C. Nerin, *J. Agric. Food Chem.*, **60**, 9842 (2012); https://doi.org/10.1021/jf302477y
38. G.E. Hoag, J.B. Collins, J.L. Holcomb, J.R. Hoag, M.N. Nadagouda and R.S. Varma, *J. Mater. Chem.*, **19**, 8671 (2009); https://doi.org/10.1039/b909148c
39. A. Gogoi, M. Navgire, K.C. Sarma and P. Gogoi, *Mater. Chem. Phys.*, **231**, 233 (2019); https://doi.org/10.1016/j.matchemphys.2019.04.013
40. G. Mamba, X.Y. Mbianda and A.K. Mishra, *Mater. Chem. Phys.*, **149-150**, 734 (2015); https://doi.org/10.1016/j.matchemphys.2014.11.035
41. J. Kaur and S. Singhal, *Superlatt. Microstruct.*, **83**, 9 (2015); https://doi.org/10.1016/j.spmi.2015.03.022
42. M. Karimi-Shamsabadi, M. Behpour, A.K. Babaheidari and Z. Saberi, *J. Photochem. Photobiol. Chem.*, **346**, 133 (2017); https://doi.org/10.1016/j.jphotochem.2017.05.038
43. M.D.G. de Luna, E.D. Flores, D.A.D. Genuino, C.M. Futalan and M.W. Wan, *J. Taiwan Inst. Chem. Eng.*, **44**, 646 (2013); https://doi.org/10.1016/j.jtice.2013.01.010
44. M. Rani, J. Yadav, Keshu and U. Shanker, *J. Colloid Interface Sci.*, **601**, 689 (2021); https://doi.org/10.1016/j.jcis.2021.05.152
45. R. Nayak, F.A. Ali, D.K. Mishra, D. Ray, V.K. Aswal, S.K. Sahoo and B. Nanda, *J. Mater. Res. Technol.*, **9**, 11045 (2020); https://doi.org/10.1016/j.jmrt.2020.07.100